Third-harmonic generation in cylindrical parabolic quantum wires with an applied electric field

Guanghui Wang*
Laboratory of Photonic Information Technology, South China Normal University, Guanghzou 510631, People's Republic of China and Laboratory of Light Transmission Optics, South China Normal University, Guangzhou 510631, People's Republic of China
(Received 9 March 2005; revised manuscript received 12 September 2005; published 27 October 2005)

The third-harmonic generation (THG) in GaAs/AlGaAs cylindrical parabolic quantum wires with an applied static-electric field is studied in detail. An analytic formula for the THG susceptibility in the model is obtained by a compact density matrix approach and an iterative procedure. Finally, the calculated results show the parabolic confinement potential and the applied electric field have great influence on the THG susceptibilities in the system. Another important point is that the maximum THG susceptibility over 10^{-9} m^2/V^2 can be obtained by optimizing the parabolic confinement potential and the applied electric field, which is over ten orders of magnitude greater than in bulk GaAs. The contributors to the very giant three-order nonlinear include the very large dipole transition matrixes and the triple resonant condition.

DOI: 10.1103/PhysRevB.72.155329 PACS number(s): 78.20.Nv, 42.65.Ky, 87.50.Rr

I. INTRODUCTION

Recently nonlinear optical properties of low-dimensional semiconductor systems such as quantum wells, quantum dots, and other nanostructures have attracted much attention in theoretical and applied physics sides.[1–14] One reason is that quantum confinement of carriers in the low-dimensional system leads to the formation of discrete energy levels and the drastic changes of physical and chemical properties such as the novel nonlinear optical effects. Another reason is that the nonlinear optical properties in the low-dimensional materials have the potential for device applications in laser amplifiers,[1] photodetectors,[2] high-speed electro-optical modulators,[3] and so on.

With recent advances in material growth techniques, such as atomic layer epitaxy, etc., the growth of single atomic layers of good quality has become possible, which has allowed potential profiles with reasonable shapes such as parabolic shapes and stepped shapes, etc. In 1983, Gurnick and De Temple[4] first discussed an asymmetric quantum well—the Morse potential well, showing that the second-order nonlinearities are 10 to 100 times larger than in bulk materials. The third-order nonlinear susceptibility, which is five orders of magnitude greater than in bulk GaAs, has been measured in coupled quantum wells by Sirtori *et al.*[5] In 1989, Chuang and Ahn[6] studied optical transitions in a parabolic quantum well with an applied electric field, and came to a conclusion that the interband optical transitions in a parabolic quantum well decrease with an increase in the electric field. In 1991, Walrod and Auyang[7] observed the large third-order optical nonlinearity due to intersubband transitions in AlGaAs/GaAs superlattices. In 1999, Sauvage and Boucaud[8] studied the third-harmonic generation (THG) in InAs/GaAs self-assembled quantum dots in both theoretical and experimental cases, and they also obtained a very large THG coefficient. Recently, Zhang and Xie[9] have studied electric field effect on the second-order nonlinear optical properties of parabolic and semiparabolic quantum wells and shown that the second-harmonic generation (SHG) susceptibility in the semiparabolic quantum well is larger than that in the parabolic quantum well for the same effective widths.

In this paper, the THG in GaAs/AlGaAs cylindrical quantum wires with a two-dimensional parabolic confinement potential and an applied uniform static-electric field is briefly studied. In Sec. II, electronic states in cylindrical coordinate systems and a simple analytical formula for THG susceptibility is derived. Numerical results and discussions are presented in Sec. III. We find that the THG susceptibility in the system is very giant and relative to the confinement potential frequency and the applied electric field. A brief summary is given in Sec. IV.

II. THEORY

Electrons in a cylindrical semiconductor quantum wire with a two-dimentional parabolic confinement potential and an applied uniform static-electric field along the x direction can be described by the effective-mass Hamiltonian in cylindrical coordinate systems as

$$H = H_r + H_z = -\frac{\hbar^2}{2m^*}\left[\frac{1}{r}\frac{\partial}{\partial r}\left(r\frac{\partial}{\partial r}\right) + \frac{1}{r^2}\frac{\partial^2}{\partial\theta^2}\right] + \frac{1}{2}m^*\omega_0^2 r^2 - eFr\cos\theta - \frac{\hbar^2}{2m^*}\frac{d^2}{dz^2}, \tag{1}$$

where $r=\sqrt{x^2+y^2}$, and m^* is the effective mass of the electron in the conduction band, ω_0 the parabolic confinement frequency, e the electron charge, and F the applied electric field.

The electronic eigenfunctions $\psi_{nm,k}$ and eigenenergies $\varepsilon_{nm,k}$, satisfying the Schrödinger equation $H\psi_{nm,k}=\varepsilon_{nm,k}\psi_{nm,k}$, are given by

$$\psi_{nm,k} = \varphi_{nm}(x,y)U_c(\mathbf{r})e^{ikz} \tag{2}$$

and

$$\varepsilon_{nm,k} = E_{nm} + \frac{\hbar^2 k^2}{2m^*}, \tag{3}$$

where k is the wave vector in the z direction and $U_c(\mathbf{r})$ is the periodic part of the Bloch function in the conduction-band bottom. φ_{nm} and E_{nm}, the envelope wave functions and the

transverse energies of the nmth subband satisfying the Schrödinger equation $H_r\varphi_{nm}=E_{nm}\varphi_{nm}$, can be written as

$$E_{nm}=(2n+|m|+1)\hbar\omega_0-\frac{e^2F^2}{2m^*\omega_0^2}, \tag{4}$$

$$\varphi_{nm}(\rho)=\sqrt{\frac{2m^*\omega_0 n!}{\hbar(n+|m|)!}}e^{-\rho^2/2}\rho^{|m|}L_n^{|m|}(\rho^2)\frac{1}{\sqrt{2\pi}}e^{im\phi}, \tag{5}$$

with

$$\rho=\sqrt{\frac{m^*\omega_0}{\hbar}\left[\left(r-\frac{eF\cos\theta}{m^*\omega_0^2}\right)^2+\left(\frac{eF\sin\theta}{m^*\omega_0^2}\right)^2\right]}, \tag{6}$$

where $n=0,1,2,\cdots$, $m=0,\pm1,\pm2,\cdots$, and $L_n^{|m|}$ are generalized Laguerre polynomials.

Let us consider a circularly polarized electromagnetic field with frequency ω incident along the z direction, interacting with the system, as follows:

$$\mathbf{E}(t)=\frac{E_0(t)}{\sqrt{2}}(\hat{e}_x\pm i\hat{e}_y), \tag{7}$$

where $\hat{e}_x$ and $\hat{e}_y$ denote the unit vectors in the x and y directions respectively, and $E_0(t)$ is expressed as

$$E_0(t)=E_0\cos(\omega t)=\tilde{E}e^{-i\omega t}+\tilde{E}e^{i\omega t}. \tag{8}$$

Then the system is excited by the electromagnetic field. By considering symmetry of Bloch states, the dipolar transition moment between the state $\psi_{nm,k}$ and $\psi_{n'm',k'}$ can be expressed as

$$\langle\psi_{nm,k}|er|\psi_{n'm',k'}\rangle=\delta_{k,k'}\langle\varphi_{nm}|er|\varphi_{n'm'}\rangle, \tag{9}$$

where δ is the Kronecker delta function.

In the following, we will derive a general expression of THG susceptibility in the two-dimensional isotropic harmonic oscillator model by the compact density-matrix method and the iterative procedure. Let a sign $\bar{\rho}$ denote the one-electron density matrix for the system. Then the evolution of which obeys the following time-dependent Liouville equation:

$$\partial\bar{\rho}_{ij}/\partial t=(i\hbar)^{-1}[H_0-erE(t),\bar{\rho}]_{ij}-\Gamma_{ij}(\bar{\rho}-\bar{\rho}^{(0)})_{ij}, \tag{10}$$

where $\bar{\rho}^{(0)}$ is the unperturbed density matrix and Γ_{ij} is the relaxation rate. For simplicity, we will assume in the following only two different Γ_{ij} values: $\Gamma_1=1/T_1$ for $i=j$ is the diagonal relaxation rate, where T_1 is the longitudinal relaxation time, and $\Gamma_2=1/T_2$ for $i\neq j$ is the off-diagonal relaxation rate, where T_2 is the transverse relaxation time. $H'=-erE(t)$ is treated as a perturbation term. Equation (10) is solved by using the usual iterative procedure,[10] then

$$\bar{\rho}(t)=\sum_n\bar{\rho}^{(n)}(t), \tag{11}$$

with

$$\frac{\partial\bar{\rho}_{ij}^{(n+1)}}{\partial t}=\frac{1}{i\hbar}\{[H_0,\bar{\rho}^{(n+1)}]_{ij}-i\hbar\Gamma_{ij}\bar{\rho}_{ij}^{(n+1)}\}-\frac{1}{i\hbar}[er,\bar{\rho}^{(n)}]_{ij}E(t). \tag{12}$$

The electronic polarization in the system may also be expanded phenomenologically as a series of the electric field. Here only the first three orders of the polarization is written down, i.e.,

$$P(t)=(\varepsilon_0\chi^{(1)}\tilde{E}e^{-i\omega t}+\varepsilon_0\chi_0^{(2)}|\tilde{E}|^2+\varepsilon_0\chi_{2\omega}^{(2)}\tilde{E}^2e^{-2i\omega t}+\varepsilon_0\chi_\omega^{(3)}|\tilde{E}|^2\tilde{E}e^{-i\omega t}+\varepsilon_0\chi_{3\omega}^{(3)}\tilde{E}^3e^{-3i\omega t})+\text{c . c .}, \tag{13}$$

where $\chi^{(1)}$, $\chi_0^{(2)}$, $\chi_{2\omega}^{(2)}$, $\chi_\omega^{(3)}$, and $\chi_{3\omega}^{(3)}$ are the linear, optical rectification, second-harmonic generation, third-order and third-harmonic generation susceptibilities, respectively. ε_0 is the vacuum dielectric constant. The electronic polarization of the nth order is given as

$$P^{(n)}(t)=\frac{1}{V}\mathrm{Tr}(\bar{\rho}^{(n)}er), \tag{14}$$

where V is the volume of interaction and Tr denotes the trace or summation over the diagonal elements of the matrix $\bar{\rho}^{(n)}er$.

In this paper we only pay attention to the THG (i.e., only consider the third-order contribution from the terms oscillating with 3ω). By using the same compact density-matrix approach and iterative procedure, the THG susceptibility per unit volume is obtained by utilizing the condition of triple resonance which can be satisfied in the parabolic potential as

$$\chi_{3\omega}^{(3)}=\frac{e^4\sigma_v}{\varepsilon_0\hbar^3}\frac{M_{01}M_{12}M_{23}M_{30}}{(\omega-\omega_{10}+i\Gamma_{10})(2\omega-\omega_{20}+i\Gamma_{20})(3\omega-\omega_{30}+i\Gamma_{30})}. \tag{15}$$

where $M_{ij}=|\langle\varphi_{j0}|r|\varphi_{i0}\rangle|$ is the off-diagonal matrix element, $\omega_{ij}=(E_{i0}-E_{j0})/\hbar$ the transition frequency, and σ_v the electronic density. For simplicity, we only consider the transitions between the quantum states of the quantum number $m=0$ in this paper.

The THG susceptibility has a resonant peak in the energy position of triple resonance, i.e., $\hbar\omega=\hbar\omega_{10}=\hbar\omega_{21}=\hbar\omega_{32}$, given by

$$\chi_{3\omega,\max}^{(3)}=\frac{e^4\sigma_v}{\varepsilon_0}\frac{M_{01}M_{12}M_{23}M_{30}}{i(\hbar\Gamma_2)^3}, \tag{16}$$

where the off-diagonal relaxation rate $\Gamma_2=\Gamma_{10}=\Gamma_{20}=\Gamma_{30}$.[15]

III. RESULTS AND DISCUSSIONS

In what follows we will discuss the THG susceptibility in GaAs/AlGaAs cylindrical parabolic quantum wires with an applied static electric field F. The parameters used in our numerical calculations are adopted as[6] $\sigma_v=10^{16}\ \mathrm{cm}^{-3}$, $T_2=0.2$ ps, $m^*=0.067m_0$ (m_0 is the mass of a free electron), the section radius of the cylindrical quantum wires $R_0=50$ nm. The relation between the parabolic confinement frequency ω_0 and R_0 must satisfy $\hbar\omega_0=\hbar^2/m^*R_0^2$.[16] So ω_0 should be much more than $6.9\times10^{11}\ \mathrm{s}^{-1}$. Given that the density of electrons and transverse relaxation time T_2, the maximum

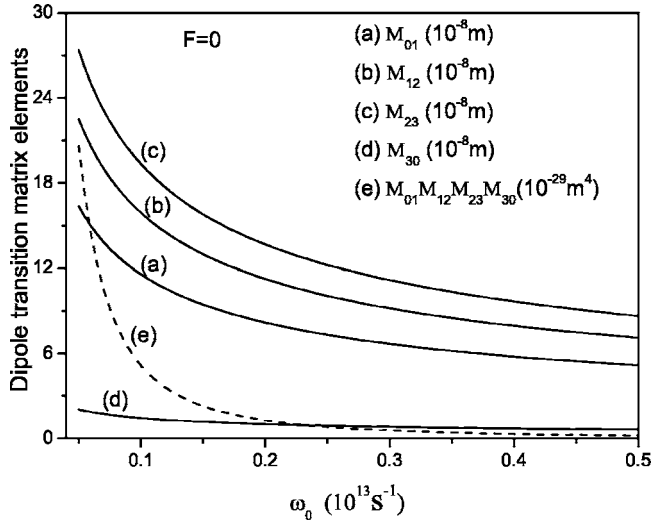

FIG. 1. The matrix elements M_{01}, M_{12},M_{23},M_{30} and their product $M_{01}M_{12}M_{23}M_{30}$ versus the parabolic confinement frequency ω_0 in the absence of an applied electric field F.

THG susceptibility $|\chi^{(3)}_{3\omega,\max}|$ at resonant peaks is determined by the geometrical factor $M_{01}M_{12}M_{23}M_{30}$, which is evident from the expression (16).

We plot the matrix elements M_{01}, M_{12}, M_{23}, M_{30} and their product $M_{01}M_{12}M_{23}M_{30}$ versus the parabolic confinement frequency ω_0 for the two cases $F=0$ in Fig. 1 and $F=2.0\times10^4$ V/m in Fig. 2. From Fig. 1, we can see easily that the matrix elements M_{01}, M_{12}, M_{23}, M_{30} and their product $M_{01}M_{12}M_{23}M_{30}$ decrease monotonously with an increase in the parabolic confinement frequency ω_0 in the absence of an applied electric field. The reason for which is that the extended areas of the intersubband wave function will decrease with an increase in ω_0, which gives rise to the electronic coherent length to be decreased. As a result, all of the dipole transition matrix elements will decrease. But in the presence of an applied electric field F, the variations of all of the

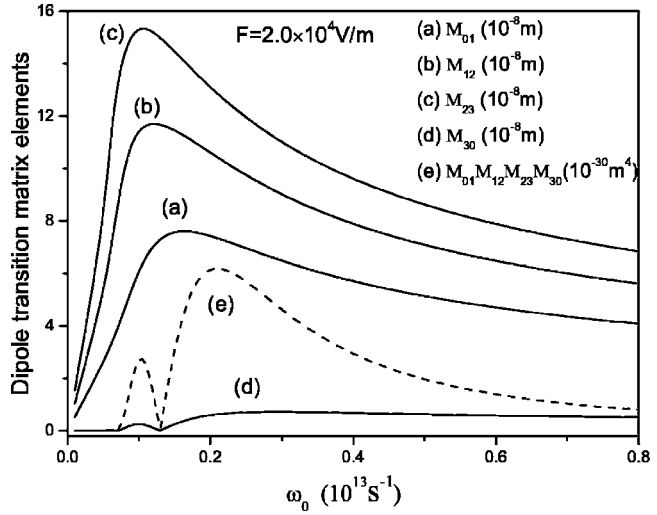

FIG. 2. The matrix elements M_{01},M_{12},M_{23},M_{30} and their product $M_{01}M_{12}M_{23}M_{30}$ versus the parabolic confinement frequency ω_0 for a fixed applied electric field F.

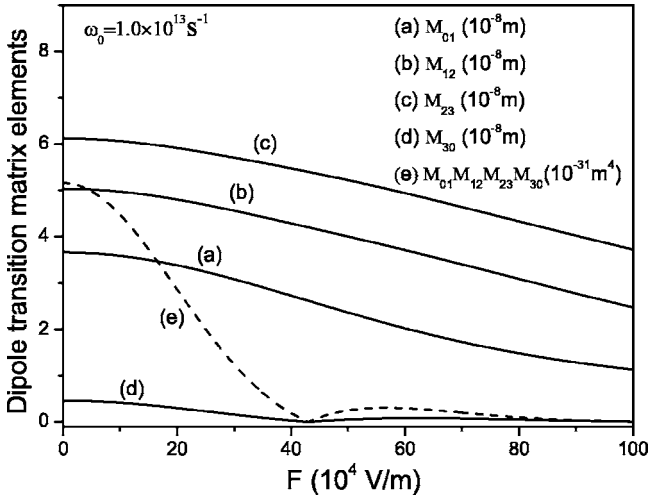

FIG. 3. The matrix elements M_{01}, M_{12}, M_{23}, M_{30} and their product $M_{01}M_{12}M_{23}M_{30}$ versus the applied electric field F for a fixed parabolic confinement frequency ω_0.

above matrix elements are obviously different from those without an applied electric field. Indeed, in Fig. 2, it is obvious that the matrix elements M_{01}, M_{12}, M_{23} increase quickly at first, and then decrease slowly with increasing ω_0, respectively. But the variation of the matrix element M_{30} appears a dip at about $\omega_0=0.13\times10^{13}$ s^{-1}, which gives rise to the product of matrix elements $M_{01}M_{12}M_{23}M_{30}$ dipping at the same ω_0. So there appear two maximum peaks in the different positions. The dip values of the matrix element M_{30} and of the product of matrix elements $M_{01}M_{12}M_{23}M_{30}$ are about 8.51×10^{-11}m and 0.11×10^{-30} m,^{4} respectively. The reason why the dip occurs is that the parabolic potential will be translated in the presence of an applied electric field F, consequently the effective scope of the intersubband wave functions in the quantum wires, in particular the high exciting-state wave function φ_{30} whose influence is the largest, will be less than one without applied electric field F. With increasing ω_0, on the one hand, the extended areas of the intersubband wave function will decrease, on the other hand, their effective scope in the quantum wires will increase, but the former is dominant, so the matrix element M_{30} will decreased. With a further increase in ω_0, however, the latter will be dominant, thereby the matrix element M_{30} will increase. But in the final analysis, the matrix element M_{30} will decrease again due to the decrease of the extended areas of the electronic wave function.

We also plot the matrix elements M_{01}, M_{12}, M_{23}, M_{30} and their product $M_{01}M_{12}M_{23}M_{30}$ versus the applied electric field F with $\omega_0=1.0\times10^{13}$ s^{-1} in Fig. 3. From Fig. 3, it is clear that the matrix elements M_{01}, M_{12}, M_{23} decrease monotonously when the electric field F increases. However, the variation of the matrix element M_{30} has a dip at about $F=43\times10^4$ V/m, which leads to the product of matrix elements $M_{01}M_{12}M_{23}M_{30}$ also appearing to dip at the same F. The dip values of the matrix element M_{30} and of the product of matrix elements $M_{01}M_{12}M_{23}M_{30}$ are about 4.78×10^{-13}m and 2.84×10^{-35} m,^{4} respectively. The reason why this dip appears is that the parabolic potential will be translated with increasing the applied electric field F, which leads to the

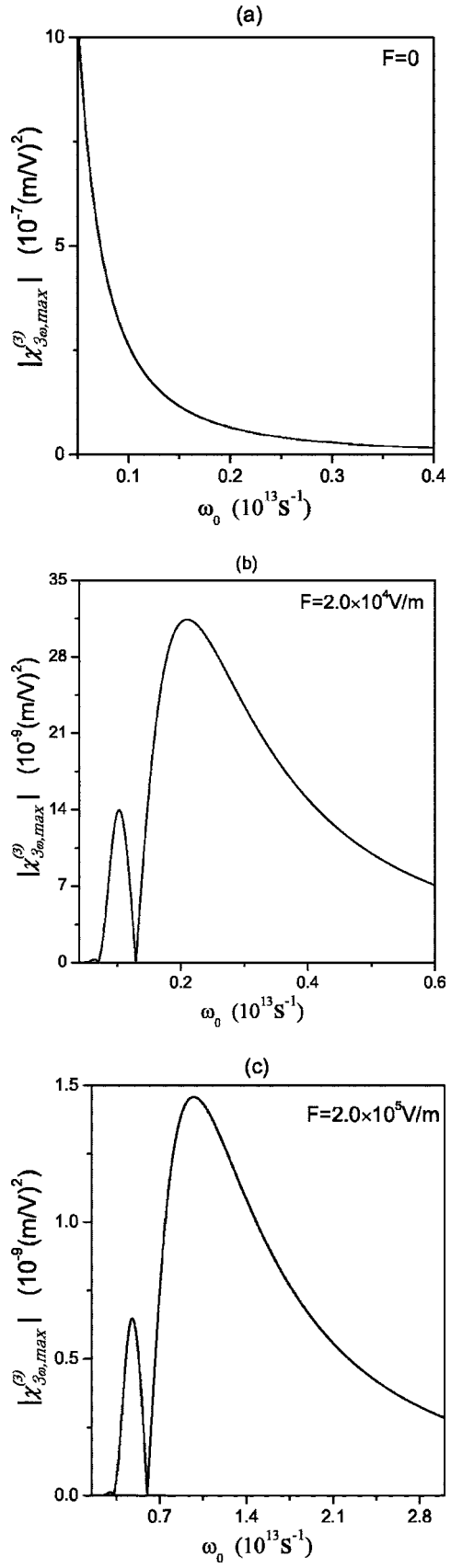

FIG. 4. The maximum THG susceptibility $|\chi^{(3)}_{3\omega,\max}|$ as a function of the parabolic confinement frequency ω_0 with $F=0$ in (a), $F=2.0\times10^4$ V/m in (b), and $F=2.0\times10^5$ V/m in (c).

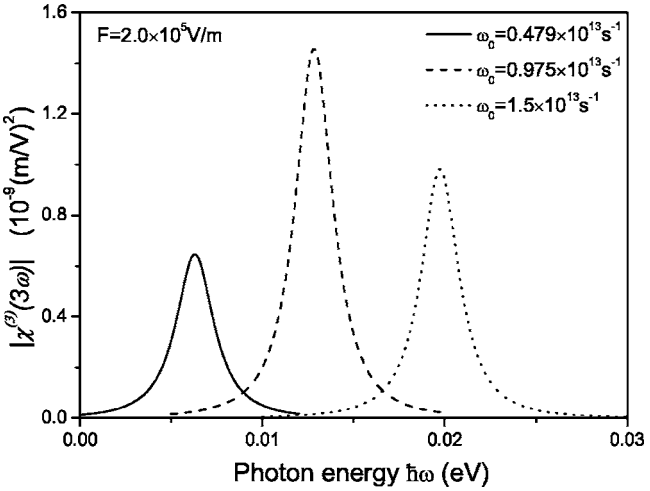

FIG. 5. The THG susceptibility $|\chi^{(3)}_{3\omega}|$ as a function of the incident photon energy $\hbar\omega$ for three different values of the parabolic confinement frequency ω_0.

effective scope of the intersubband wave functions in the quantum wires will decrease. Therefore the relative matrix element M_{30} first decrease. With a further increase in F, however, the parabolic potential will be gradually translated into the semiparabolic potential, so the M_{30} will increase. But which will decrease finally due to the decrease of the effective scope of the electronic wave functions in the quantum wires.

Figure 4 shows the maximum THG susceptibility $|\chi^{(3)}_{3\omega,\max}|$ at resonant peaks as a function of the parabolic confinement frequency ω_0 with $F=0$ in Fig. 4(a), $F=2.0\times10^4$ V/m in Fig. 4(b), and $F=2.0\times10^5$ V/m in Fig. 4(c). From Fig. 4(a), we can see that the maximum THG susceptibility decreases monotonously with increasing ω_0 in the absence of an applied electric field. In Figs. 4(b) and 4(c), however, it is distinct that the variation of the maximum THG susceptibility is very large and there appear two maximum peaks in the presence of an applied electric field, which is consistent with those of the product of matrix elements $M_{01}M_{12}M_{23}M_{30}$ in Fig. 2. When $F=2.0\times10^4$ V/m, the two maximum peaks occur at $\omega_0=0.103\times10^{13}$ s^{-1} and 0.21×10^{13} s^{-1}, respectively. But when $F=2.0\times10^5$ V/m, they occur at $\omega_0=0.479\times10^{13}$ s^{-1} and $0.975\times10^{13}s^{-1}$, respectively. From Figs. 4(b) and 4(c), we can also find that the maximum THG susceptibility decreases to original 4.6% when the external electric field F increases 10 times from 2.0×10^4 to 2.0×10^5 V/m. Therefore the THG susceptibility is sensitive to the applied electric field in the model.

Figure 5 shows the THG susceptibility $|\chi^{(3)}_{3\omega}|$ as a function of the incident photon energy $\hbar\omega$ for three different values of the parabolic confinement frequency ω_0: (a) $\omega_0=0.479\times10^{13}$ s^{-1}, (b) $\omega_0=0.975\times10^{13}$ s^{-1}, and (c) $\omega_0=1.5\times10^{13}$ s^{-1} with $F=2.0\times10^5$ V/m, which are illustrated by the solid, dashed, and dotted line, respectively. From Fig. 5, It can be easily seen that ω_0 has great influence on the THG susceptibility $|\chi^{(3)}_{3\omega}|$, whose variation at resonant peaks is identical with those in Fig. 4(c), and three resonant peaks occur at $\hbar\omega=0.0063$, 0.013, 0.020 eV, respectively. A very important property is that the resonant peak will move to the

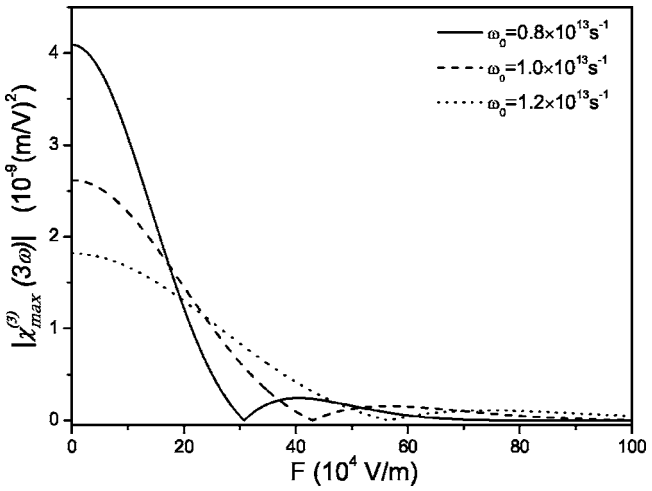

FIG. 6. The maximum THG susceptibility $|\chi^{(3)}_{3\omega,\max}|$ as a function of the applied electric field F for three different parabolic confinement frequencies.

right side of the curve with ω_0 increase, which predicts a strong confinement-induced blueshift in semiconductor quantum wires. The physical origin of the shift is the quantum confinement effect in these nanostructures, which causes the separation of energy levels, and the stronger the confinement effect is, the broader the separation will be.

Figure 6 shows the maximum THG susceptibility $|\chi^{(3)}_{3\omega,\max}|$ at resonant peaks as a function of the applied electric field F with three different parabolic confinement frequencies (a) $\omega_0=0.8\times10^{13}$ s^{-1}, (b) $\omega_0=1.0\times10^{13}$ s^{-1}, (c) $\omega_0=1.2\times10^{13}$ s^{-1}, which are illustrated by the solid, dashed, and dotted lines, respectively. From Fig. 6, we can find the magnitude of the resonant peaks is different with the different ω_0 and F. At $F=0$, the magnitude of the resonant peaks is the largest, and the weaker the parabolic confinement potential is, the larger the resonant peaks of the THG susceptibility will be. The minimum resonant peak values are 1.31×10^{-12}, 1.44×10^{-13}, and 2.60×10^{-13} m^2/V^2 for three groups of parameters (a) $\omega_0=0.8\times10^{13}$ s^{-1}, $F=30.75\times10^4$ V/m, (b) $\omega_0=1.0\times10^{13}$ s^{-1}, $F=43\times10^4$ V/m, and (c) $\omega_0=1.2\times10^{13}$ s^{-1}, $F=56.55\times10^4$ V/m, respectively.

From Figs. 4–6, we can see that the maximum THG susceptibility may be obtained over 10^{-9} m^2/V^2 by optimizing the values of ω_0 and F, which is much larger than the calculated value 1.3×10^{-14} m^2/V^2 and the measured value 0.9×10^{-14} m^2/V^2 for coupled quantum wells of AlInAs/GaInAs by Carlo Sirtori *et al.*,[5] and is over ten orders of magnitude greater than in bulk GaAs materials. The enhancement of the third-order nonlinearities in the cylindrical parabolic quantum wires stems from the quantum confinement effects and from the band structure, satisfying the triple resonance conditions, of this system. These properties make these model potential materials be very promising candidates for the application of optical devices.

IV. SUMMARY

In this paper, the THG in GaAs/AlGaAs cylindrical parabolic quantum wires with an applied uniform static-electric field is investigated in detail. The calculated results show that the parabolic confinement frequency ω_0 and the applied electric field F have great influence on the THG susceptibility. Another important point is that very large THG susceptibility over 10^{-9} m^2/V^2 can be got by optimizing the parabolic confinement potential and the applied electric field. The contributors to the very giant three-order nonlinear include the very large dipole transition matrixes, and the triple resonant condition. Therefore, the properties may have profound consequences as regards improvements of optical devices such as ultrafast optical switches and optical communications.

ACKNOWLEDGMENTS

This work was supported by the Natural Science Foundation of Guangdong Province, China, under Grant Nos. 5005918 and 04105804, and the National Natural Science Foundation, China, under Grant No.10474023.

*Email address: scnuwgh@163.com

[1] R. F. Kazarinov and R. A. Suris, Sov. Phys. Semicond. **5**, 707 (1971).
[2] F. Capasso, K. Mohammed, and A. Y. Cho, IEEE J. Quantum Electron. **QE-22**, 1853 (1986).
[3] A. B. Miller, Int. J. High Speed Electron. Syst. **1**, 19 (1991).
[4] M. K. Gurnick and T. A. DeTemple, IEEE J. Quantum Electron. **QE-19**, 791 (1983).
[5] Carlo Sirtori, *et al.*, Phys. Rev. Lett. **68** , 1010 (1992).
[6] S. L. Chuang and D. Ahn, J. Appl. Phys. **65**, 2822 (1989).
[7] D. Walrod *et al.*, Appl. Phys. Lett. **59**, 2932 (1991).
[8] S. Sauvage *et al.*, Phys. Rev. B **59**, 9830 (1999).
[9] Li Zhang and Hong-jing Xie, Phys. Rev. B **68**, 235315 (2003).
[10] E. Rosencher and Ph. Bois, Phys. Rev. B **44**, 11 315 (1991).
[11] Eiichi Hanamura, Phys. Rev. B **37**, 1273 (1988).
[12] J. E. Sipe and A. I. Shkrebtii, Phys. Rev. B **61**, 5337 (2000).
[13] A. Vasanelli, R. Ferreira, H. Sakaki, and G. Bastard, Solid State Commun. **118**, 459 (2001).
[14] Guanghui Wang and Guo KangXian, Physica B **315**, 234 (2002).
[15] The homogeneous linewidth corresponding to the three denominator terms in Eq. (15) are adopted reasonably due to the particular band structure in parabolic potential and the δ-like density of states in quantum wires and quantum dots, as explained in Ref. 8.
[16] Weiming Que, Phys. Rev. B **45**, 11 036 (1992).